360 Panorama Super-resolution using Deep Convolutional Networks

Vida Fakour-Sevom[1,2], Esin Guldogan[1] and Joni-Kristian Kämäräinen[2]
[1]*Nokia Technologies, Finland*
[2]*Laboratory of Signal Processing, Tampere University of Technology, Finland*

Keywords: Super-resolution, Virtual Reality, Equirectangular Panorama, Deep Convolutional Neural Network.

Abstract: We propose deep convolutional neural network (CNN) based super-resolution for 360 (equirectangular) panorama images used by virtual reality (VR) display devices (e.g. VR glasses). Proposed super-resolution adopts the recent CNN architecture proposed in (Dong et al., 2016) and adapts it for equirectangular panorama images which have specific characteristics as compared to standard cameras (e.g. projection distortions). We demonstrate how adaptation can be performed by optimizing the trained network input size and fine-tuning the network parameters. In our experiments with 360 panorama images of rich natural content CNN based super-resolution achieves average PSNR improvement of 1.36 dB over the baseline (bicubic interpolation) and 1.56 dB by our equirectangular specific adaptation.

1 INTRODUCTION

Super-resolution (SR) is one of the actively investigated problems of image processing where the main objective is to recover the original high resolution (HR) image from a low resolution (LR) one(s) (Yang et al., 2014). Due to the limitation in the available information, loss of details, super-resolution is generally an ill-posed problem. Super-resolution algorithms are divided into two main groups: Multi-frame SR (Hung and Siu, 2009; Btz et al., 2016) (traditional method) which exploit information available in multiple frames and Single Image Super-resolution (SISR) (Tang and Chen, 2013; Tsurusaki et al., 2016; Cheng et al., 2017) which tries to recover original information from a single image. The SISR methods are further divided into Learning-based and Interpolation-based methods. In this paper, we focus on the learning-based single image super-resolution.

Freeman (Freeman et al., 2002) introduced the concept of learning-based super-resolution for the first time and proposed an example-based method. In (Yang et al., 2008) the authors presented sparse coding based SR using sample images for training an over-complete dictionary. Recently, deep learning has set the state-of-the-arts in many computer vision tasks including super-resolution (Ji et al., 2016; Dong et al., 2016), denoising and removing artifacts (Quijas and Fuentes, 2014; Ji et al., 2016).

360 panorama images and videos have recently gained momentum due to availability of consumer level display devices such as Samsung Gear VR and HTC Vive VR. The users are used to experience high quality and high resolution images and videos due to availability of professional level sensors such as high-end Nokia OZO capturing device which uses 8 wide angle lenses and provides 4K image per eye. The captured videos/images are stitched together to make a single content which might suffer from stitching artifacts. Moreover, an equirectangular panorama image is generated very differently than traditional images. Equirectangular panorama mapping takes spherical input and maps the latitude and longitude coordinates onto a single rectangular plane. This may cause strong distortions on the produced image (equirectangular panorama projection). Therefore, it is interesting to study whether the previous SR methods still work or do they need special adaptation.

In this work we adopt the deep convolutional neural network super-resolution approach by Dong et al. (Dong et al., 2016) (SRCNN) to recover high-resolution 360 (equirectangular) panorama images from their low resolution versions. We adapt the existing methodology by studying the effects of input sub-image size to the network and fine-tuning with the different number of iterations on 360 panorama dataset. In our experiments the SRCNN provides clear improvement as compared to the baseline (bicubic interpolation) and our adaptation techniques further improve the results.

Fakour-Sevom, V., Guldogan, E. and Kämäräinen, J-K.
360 Panorama Super-resolution using Deep Convolutional Networks.
DOI: 10.5220/0006618901590165
In *Proceedings of the 13th International Joint Conference on Computer Vision, Imaging and Computer Graphics Theory and Applications (VISIGRAPP 2018) - Volume 4: VISAPP*, pages 159-165
ISBN: 978-989-758-290-5

Contributions – The novel contributions of our work are:

- We demonstrate effective learning-based super-resolution for 360 (equirectangular) panorama images by adopting the recent SRCNN method for standard images.
- We adapt the methodology to the characteristics of high-resolution 360 panorama images by optimizing the network input size and fine-tuning with 360 panorama training set.
- We create a dataset to benchmark 360 degree panorama image super-resolution methods.

2 RELATED WORK

Image Super-resolution (SR) – Addressing the problem of recovering a HR image from a given LR image is known as single image super-resolution. In many works, SISR is divided into *Learning-based* and *Interpolation-based* methods (Zhou et al., 2012). In early interpolation-based methods, it is assumed that a LR input image is the downsized version of a HR image. Hence, the HR image, considering aliasing, is recovered from upscaling the LR input image (Siu and Hung, 2012). Currently, learning-based approaches are widely used in order to make a mapping function between LR images and their corresponding HR ones. Freeman in (Freeman et al., 2002) for the first time introduced the concept of learning-based super-resolution and proposed an example-based method. The main idea behind the learning-based approach is using the spatial similarities between Low-Resolution and High-Resolution images and making a mapping function in order to predict the HR image for a given LR input image. Methods in (Yang et al., 2008; Timofte et al., 2013) use a learned over-complete dictionary based on sparse signal representation. The main idea is based on the assumption of existing the same sparse coefficient in LR and their corresponding HR patches.

Deep CNN SR – Lately, Convolutional Neural Network (CNN) approaches have been popular in many vision applications including super-resolution (Cui et al., 2014; Shi et al., 2016; Kim et al., 2016; Schulter et al., 2015) where they had noticeable performance improvements over the previous state-of-the-arts.

SRCNN (Dong et al., 2016), known as a representative state-of-the-art method for deep learning, applies a single image super-resolution where the network end-to-end learns a mapping between LR and HR images. Moreover, it is shown that existing sparse coding methods might be considered as a deep learning. In (Ji et al., 2016), a HR image is created over iterative refinement and back projection methods. An extension of SRCNN method is seen in (Youm et al., 2016) where a single system's input is replaced by a multi-channel one. In this method the input contains original LR image, corresponding edge-enhanced and interpolated ones. Single image super-resolution using deep learning and gradient transformation is another recent approach proposed in (Chen et al., 2016). In their extension, closest gradient to the one in the original image is estimated by transforming observed gradient in the upscaled images using a gradient transformation network.

3 DEEP MULTI-RESOLUTION

In our work we utilized the deep super-resolution convolutional neural network architecture by (Dong et al., 2016) since it recently demonstrated state-of-the-art accuracy for various datasets and over many competitive non-CNN based competitors. The main idea of SRCNN is to learn a mapping from low resolution images to high resolution images by devising a suitable network structure and error function, and then train the network with a large dataset.

In our case, the main target is to input a low-resolution equirectangular panorama image to the SR model and reconstruct its corresponding high-resolution version. In the training phase, we input multi-resolution input sub-images (the network training input is not the whole image but randomly cropped regions called as *sub-images*) to the network in order to study the effect of multi-resolution sub-images on the super-resolution results. It is likely that equirectangular panorama exhibits different characteristics to standard images and therefore requires adaptation.

The first step in SRCNN is to perform a standard bicubic interpolation for the input image of any size (denoted as X) to the desired output size of the HR image: $f : X \rightarrow Y$. The aim of the next CNN forward pass step is to recover the high resolution details for Y to make an image (denoted as $F(\mathrm{Y})$) that is similar to the original high quality image. The desired above-mentioned mapping function (denoted as F) is composed of the three convolution layers: *patch extraction*, *non-linear mapping* and *reconstruction*.

In the first layer the patches are extracted by convolving the image with a set of filters. Afterwards, the patches are represented using a set of pre-trained bases. The first layer is shown as an operation F_1:

$$F_1(Y) = max(0, W_1 * Y + B_1) \qquad (1)$$

where $*$ denotes convolution, moreover, W_1 and B_1 show the filters and biases, respectively. Assuming c as a number of channels of an image and f_1 as a filter size, n_1 convolutions with the kernel size of $c \times f_1 \times f_1$ are applied on the image. Each element of the n_1-dimensional B_1 vector is corresponding to a filter individually. Hence, extracting an n_1-dimensional feature for each patch is the final output of this step.

In the second layer, other n_2-dimensional vectors are created from the mapped n_1-dimensional vectors (previous step). The corresponding operation is:

$$F_2(Y) = max(0, W_2 * F_1(Y) + B_2) \quad (2)$$

where W_2 and B_2 correspond to the first layer equation filters and biases, respectively. However this time there are n_2 filters of size $n_1 \times f_2 \times f_2$ and n_2-dimensional B_2 vector. Eventually, the output of this layer is a high-resolution patch which will be used for the next layer i.e. reconstruction.

In the last layer, a convolutional layer is defined where the final high-resolution image is produced:

$$F(Y) = W_3 * F_2(Y) + B_3 \quad (3)$$

where W_3 is c filters of size $n_2 \times f_3 \times f_3$ and B_3 is a c-dimensional vector. Minimizing the loss between reconstructed images and ground truth image makes estimating the above-mentioned parameters, i.e. $W_1, W_2, W_3, B_1, B_2, B_3$ possible. These parameters are needed for learning the mapping function. Mean Square Error is used as the network loss function:

$$L(\theta) = \frac{1}{n} \sum_{i=1}^{n} \|F(Y_i; \theta) - X_i\|^2, \quad (4)$$

where $\theta = \{W_1, W_2, W_3, B_1, B_2, B_3\}$, n is the number of training images.

3.1 Training

The three mentioned steps together result the SRCNN convolutional neural network. Training is performed by cropping training images (X_i) to random $f_{sub} \times f_{sub}$-pixel sub-images (in experimental part we use various sizes). Low-resolution samples are created by downscaling and upscaling the sub-images after making them blurred using Gaussian kernel. The downscaling and upscaling are completed via Bicubic interpolation where the same scaling factor (in our experiments is 3) is used. In order to avoid the border effect, padding is not used in the network. Hence, the output size of a sub-image based on the network filter sizes ($(f_{sub} - f_1 - f_2 - f_3 + 3)^2 \times c$) is smaller than the input size. Training model is implemented using *Caffe* package which is also used in our implementation. Once training is done and network parameters are created, the SRCNN trained model is applied to test images of any size.

4 EXPERIMENTS

We first experimented our equirectangular panorama images with the existing training model (using original training and test images). Next, we examined the training phase with our own images and studied the effect of using equirectangular images instead of the traditional ones on the results. Subsequently, the training parameters, number of iterations and network input sub-image size, are adaptively changed based on our images.

4.1 Data

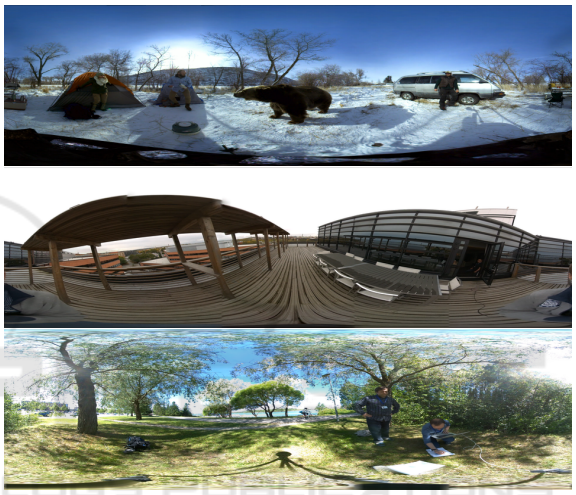

Figure 1: Video frames of the size 3840×1081 captured using a Nokia OZO high-end VR camera.

The dataset which we use consists of 34 high quality equirectangular panorama images which are single frames of various 360-video scenes captured using a Nokia OZO VR camera[1] (Figure 1). For comparison, the small training set, used in the original paper, with 91 images is used. The sub-images size is set to a fixed size i.e. $f_{sub} = 33$ in SRCNN, but in our experiments two $f_{sub} = 65$ and $f_{sub} = 129$ are also studied. The sub-images are extracted from the ground truth images with a stride of 14 (same as default setting in the original paper for $f_{sub} = 33$) and then we increase it to 30 and 62, for $f_{sub} = 65$ and $f_{sub} = 129$, respectively.

4.2 Settings

The baseline model in our experiments is the original network proposed in (Dong et al., 2016) which uses 33×33 sub-image input and their own dataset

[1] https://ozo.nokia.com/vr/

Table 1: Super-resolution results for all 34 frames from 5-fold cross-validation where 6-7 images selected for the test set. Bicubic results correspond to bicubic interpolation, SRCNN is (Dong et al., 2016) and SRCNN-ft is fine-tuned with our equirectangular panorama data using the original settings (33×33 patch size) and after 15 million fine tuning iterations.

	PSNR (dB)		
Frame#	*Bicubic*	*SRCNN*	*SRCNN-ft*
F01	34.38	35.26	35.43
F02	30.13	31.24	31.46
F03	23.13	23.56	23.66
F04	30.44	32.36	32.51
F05	35.79	36.50	36.54
F06	32.24	33.35	33.48
F07	38.97	40.12	40.28
F08	28.02	28.98	29.19
F09	34.70	35.59	35.69
F10	28.14	29.12	29.32
F11	27.18	28.14	28.29
F12	30.54	32.50	32.70
F13	34.74	37.12	37.18
F14	32.20	33.29	33.40
F15	38.94	40.48	41.17
F16	37.49	39.15	39.60
F17	40.09	41.04	42.02
F18	23.16	23.68	23.83
F19	33.78	34.78	34.91
F20	28.54	29.68	29.79
F21	27.52	28.22	28.28
F22	41.39	42.82	42.98
F23	32.32	33.46	33.65
F24	38.67	40.23	40.52
F25	36.31	38.62	38.67
F26	35.56	37.89	38.08
F27	35.69	37.57	37.63
F28	40.95	42.54	42.69
F29	36.01	38.02	38.28
F30	37.55	38.91	39.47
F31	33.59	34.72	34.91
F32	32.53	34.59	34.69
F33	32.98	34.59	34.72
F34	33.03	34.68	34.79
avg. improv. [dB]	-	1.36	1.56
avg. improv. [%]	-	4.1%	4.7%

for training the model with batch size 128 The network settings are: $c = 3$, $f_1 = 9$, $f_2 = 1$, $f_3 = 5$, $n_1 = 64$ and $n_2 = 32$. The results have been evaluated with the scaling factor equal to 3. For our experiment we downscaled the original images by the factor of 3, meaning that the input image is subsampled and the resolution is one third of the initial size in horizontal and vertical directions, then it is again upsampled by the factor of 3 to the initial size.

We conducted our experiments using 5-fold cross-validation and the results for single images have been selected from the folds where these images were not used in training. For our experiments we tested fine-tuning the original network with equirectangular panorama images for 5, 10, 15, 20 and 30 million iterations keeping the original batch size and using various network input sub-image sizes (33×33, 65×65 and 129×129). For the largest sub-image size we decreased the learning rate from 0.0001 to 0.00001 to avoid overfitting. As our performance measure we report the peak signal-to-noise ration (PSNR) defined in decibels (dB). Moreover, we report also bicubic interpolation as the baseline method to epmhasize overall superiority of deep learning based super-resolution.

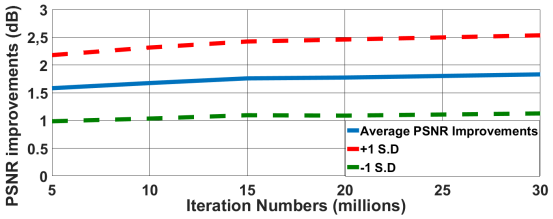

Figure 2: Average and plus/minus one standard deviation movement of SR improvement (dB) over all equirectangular panorama images as the function of the number of fine-tuning iterations. The average training time takes roughly 11 hours for 5M iterations running on NVIDIA GEForce GTX980 GPU.

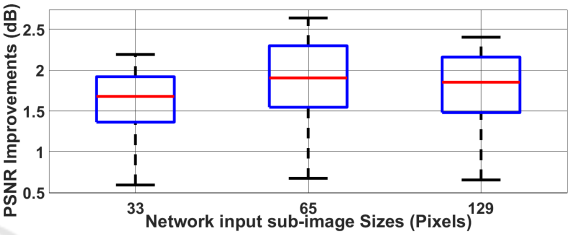

Figure 3: Box plots of the average PSNR improvements for SR with different network input sub-image sizes.

4.3 Results

Using the standard SRCNN for our equirectangular dataset improved the results quite significantly ($+1.36dB$/$+4.1\%$) as compared to the baseline (see Table 1) and in the remaining experiments we investigated the different adaptation strategies.

Fine-tuning – In the first experiment we fine-tuned the SRCNN network with our equirectangular panorama images. Note that the images are from different video clips and therefore there is no immediate correlation between the contents. Fine tuning was performed 15 million iterations with the original learning rate 0.0001 and using the original sub-image input size and batch size The results are reported for 5-fold cross-validation where image specific numbers are taken as averages from folds where that image was only in the test set. The results for the fine-tuned network (SRCNN-FT) are shown in Table 1. For all images the SR results improved and demonstrated the average improvement $1.36dB \rightarrow 1.56dB$

(a) A high density equirectangular panorama image captured using a Nokia OZO VR camera.

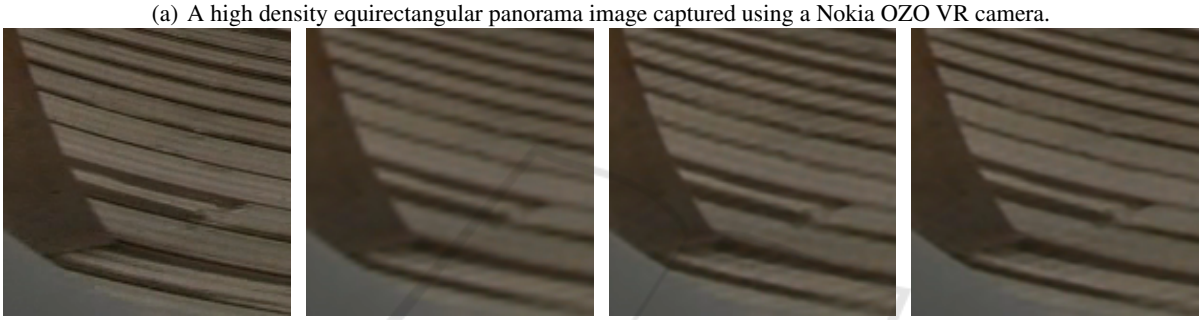

(b) Original (c) Bicubic / 31.15 dB (d) SRCNN / 31.74 dB (e) SRCNN_FT / 32.95 dB

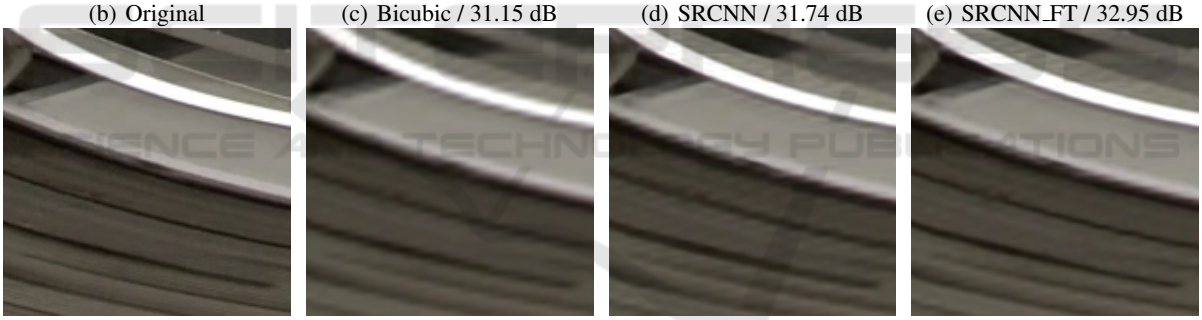

(f) Original (g) Bicubic / 30.67 dB (h) SRCNN / 33.49 dB (i) SRCNN_FT / 34.53 dB

Figure 4: Equirectangular panorama super-resolution examples.

over all contents. Clearly the fine-tuning is beneficial for the process as the network learns equirectangular specific characteristics such as the lens distortion which is very strong vertically.

Number of Iterations – In this experiment we kept the network structure fixed to the same as the previous one, but experimented the limits of fine-tuning by increasing the number of iterations. In Figure 2 the average and standard deviation of SR improvement are shown in dB over all images. It is noteworthy that the improvement continues beyond 15 million iterations and reaches improvement $1.56dB$ which is significantly better than with the original SRCNN ($1.34dB$).

Network Input Sub-image Size – In this experiment we fixed the network structure and parameters and kept the number of iterations 15M and then applied the multi-resolution sub-image experiment. The sub-image sizes are changed from 33×33 to 65×65 and 129×129. The PSNR box plots for the average improvements as compared to the bicubic baseline are shown in Figure 3. It is noteworthy that there is clear improvement from the sub-image size from 33×33 to 65×65, but the results got worse with the larger sub-image size of 129×129. In general, the results should improve for large sub-image sizes, but then the network becomes more sensitive to overfitting and therefore results got worse.

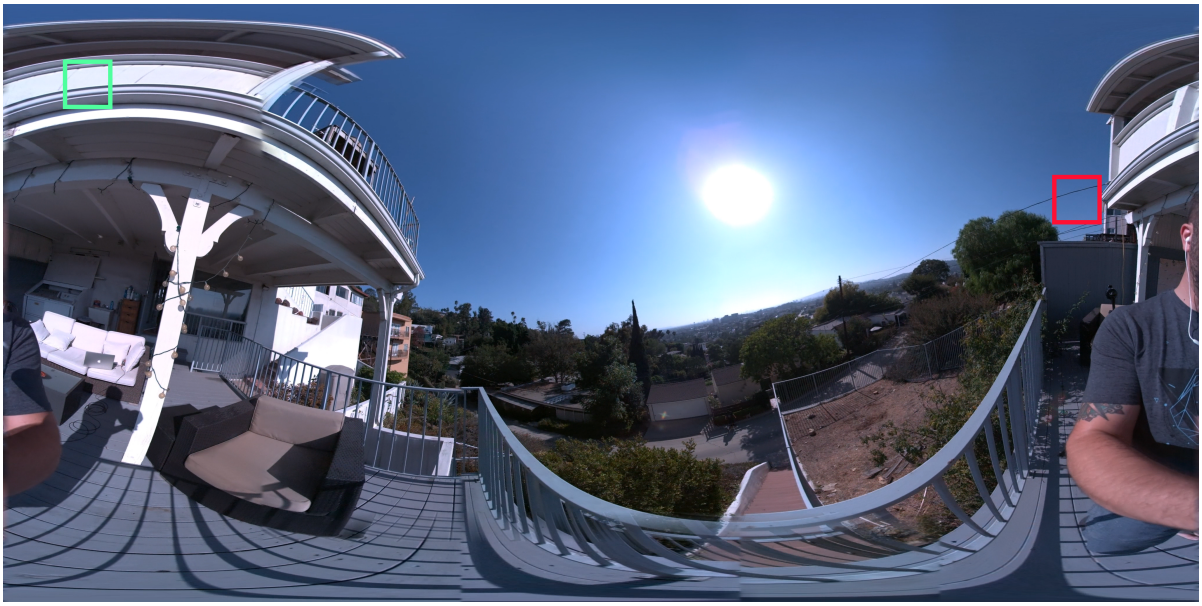

(a) A high density equirectangular panorama image captured using a Nokia OZO VR camera.

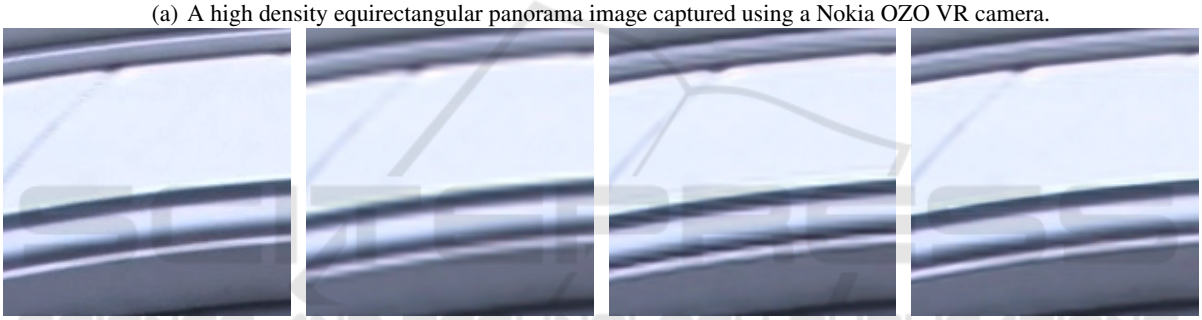

(b) Original (c) Bicubic / 30.53 dB (d) SRCNN / 32.68 dB (e) SRCNN_FT / 35.52 dB

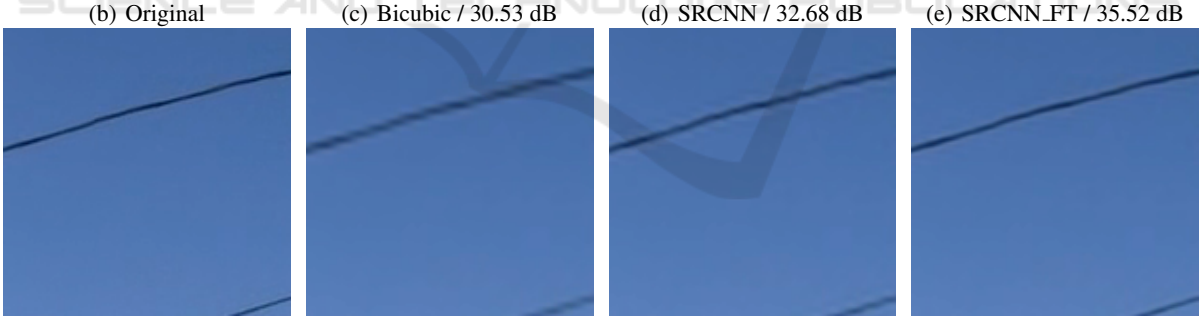

(f) Original (g) Bicubic / 36.22 dB (h) SRCNN / 38.6535 dB (i) SRCNN_FT / 42.28 dB

Figure 5: Equirectangular panorama super-resolution examples.

4.4 Examples

Visual comparison of the applied Bicubic interpolation and super-resolution images using SRCNN and SRCNN_FT are given in Figure 4-5. Two random regions, with the size of 150×150, are extracted from our three input equirectangular images. Applying Bicubic, SRCNN and SRCNN_FT showed that the SRCNN method has a high accuracy in terms of sharpness and removing artifacts to the baseline (bicubic interpolation). Our multi-resolution fine-tuned SRCNN makes notable improvements over SRCNN by equirectangular specific adaptation.

5 CONCLUSIONS

We proposed a learning-based super-resolution method for equirectangular panorama images by adopting the recently introduced deep convolutional neural network based super-resolution architecture

SRCNN. We investigated the different parameters of the architecture for equirectangular panorama images and showed how special adaptation by larger network input layer sub-images and dedicated fine-tuning improve the results as compared to the baseline (bicubic interpolation) and also to the original SRCNN. In our future work we will develop novel VR applications of image super-resolution.

REFERENCES

Btz, M., Koloda, J., Eichenseer, A., and Kaup, A. (2016). Multi-image super-resolution using a locally adaptive denoising-based refinement. In *2016 IEEE 18th International Workshop on Multimedia Signal Processing (MMSP)*, pages 1–6.

Chen, J., He, X., Chen, H., Teng, Q., and Qing, L. (2016). Single image super-resolution based on deep learning and gradient transformation. In *2016 IEEE 13th International Conference on Signal Processing (ICSP)*, pages 663–667.

Cheng, P., Qiu, Y., Wang, X., and Zhao, K. (2017). A new single image super-resolution method based on the infinite mixture model. *IEEE Access*, 5:2228–2240.

Cui, Z., Chang, H., Shan, S., Zhong, B., and Chen, X. (2014). Image super-resolution as sparse representation of raw image patches. In *2014 Computer Vision-ECCV*, pages 49–64.

Dong, C., Loy, C., He, K., and Tang, X. (2016). Image super-resolution using deep convolutional networks. *IEEE Trans. on PAMI*, 38(2).

Freeman, W. T., Jones, T. R., and Pasztor, E. C. (2002). Example-based super-resolution. *IEEE Computer Graphics and Applications*, 22(2):56–65.

Hung, K.-W. and Siu, W. C. (2009). New motion compensation model via frequency classification for fast video super-resolution. In *2009 16th IEEE International Conference on Image Processing (ICIP)*, pages 1193–1196.

Ji, X., Lu, Y., and Guo, L. (2016). Image super-resolution with deep convolutional neural network. In *2016 IEEE First International Conference on Data Science in Cyberspace (DSC)*, pages 626–630.

Kim, J., Lee, J. K., and Lee, K. M. (2016). Accurate image super-resolution using very deep convolutional networks. In *2016 IEEE Conference on Computer Vision and Pattern Recognition (CVPR)*, pages 1646–1654.

Quijas, J. and Fuentes, O. (2014). Removing jpeg blocking artifacts using machine learning. In *2014 Southwest Symposium on Image Analysis and Interpretation*, pages 77–80.

Schulter, S., Leistner, C., and Bischof, H. (2015). Fast and accurate image upscaling with super-resolution forests. In *2015 IEEE Conference on Computer Vision and Pattern Recognition (CVPR)*, pages 3791–3799.

Shi, W., Caballero, J., Huszr, F., Totz, J., Aitken, A. P., Bishop, R., Rueckert, D., and Wang, Z. (2016). Real-time single image and video super-resolution using an efficient sub-pixel convolutional neural network. In *2016 IEEE Conference on Computer Vision and Pattern Recognition (CVPR)*, pages 1874–1883.

Siu, W. C. and Hung, K. W. (2012). Review of image interpolation and super-resolution. In *Proceedings of The 2012 Asia Pacific Signal and Information Processing Association Annual Summit and Conference*, pages 1–10.

Tang, Y. and Chen, H. (2013). Matrix-value regression for single-image super-resolution. In *2013 International Conference on Wavelet Analysis and Pattern Recognition*, pages 215–220.

Timofte, R., De, V., and Gool, L. V. (2013). Anchored neighborhood regression for fast example-based super-resolution. In *2013 IEEE International Conference on Computer Vision*, pages 1920–1927.

Tsurusaki, H., Kameda, M., and Ardiansyah, P. O. D. (2016). Single image super-resolution based on total variation regularization with gaussian noise. In *2016 Picture Coding Symposium (PCS)*, pages 1–5.

Yang, C.-Y., Ma, C., and Yang, M.-H. (2014). *Single-Image Super-Resolution: A Benchmark*, pages 372–386. Springer International Publishing, Cham.

Yang, J., Wright, J., Huang, T., and Ma, Y. (2008). Image super-resolution as sparse representation of raw image patches. In *2008 IEEE Conference on Computer Vision and Pattern Recognition*, pages 1–8.

Youm, G. Y., Bae, S. H., and Kim, M. (2016). Image super-resolution based on convolution neural networks using multi-channel input. In *2016 IEEE 12th Image, Video, and Multidimensional Signal Processing Workshop (IVMSP)*, pages 1–5.

Zhou, F., Yang, W., and Liao, Q. (2012). Interpolation-based image super-resolution using multisurface fitting. *IEEE Transactions on Image Processing*, 21(7):3312–3318.